32nd URSI GASS, Montreal, 19-26 August 2017

Radio-Propagation-Measurement-Based Calculations of Multi-User Distributed MIMO Channel Capacity for a Small Cluttered Room at 2 GHz, 18 GHz and 28 GHz

Mohamad Alkadamani and Robert J.C. Bultitude
Dept. of Systems and Computer Engineering
Carleton University, Ottawa, Canada

Abstract

This paper reports multi-user D-MIMO channel capacity calculations for 4x4 D-MIMO channels simulated using transmission loss and shadowing models derived from channel sounding measurements made with a vector-network-analyser (VNA) based channel sounding system. The channel sounding measurements were made with a bandwidth of 500 MHz at centre frequencies of 2.4 GHz, 18 GHz, and 28 GHz, in a small cluttered study room. Transmission was from an emulated sector antenna mounted with a downtilt of 62.5 degrees, above the suspended ceiling in the room at a height of 4 m above floor level. Reception was at 45 desk-top-height locations scattered throughout the room using an omni directional antenna at 2.4 GHz, and a step-wise azimuth and elevation scanning horn antenna with 10 deg. beamwidths in both planes at 18 GHz and 28 GHz.

Reported results show that, since transmission loss differences and shadowing on the Tx-Rx links dominate over fast fading characteristics, given the same coverage-area-averaged SNR, equivalent capacities would be realised at 2 GHz and at 18 GHz, given omni directional UE antennas at 2 GHz and UEs with antenna beams that can be steered so as to receive the maximum power at 18 GHz. Further, since measurement results show that powers near the maximum would often be received with UE antennas pointed in one of several different directions, if such steering can mitigate shadow correlations at 18 GHz, a capacity gain of about 1 bit/S/Hz could be achieved at 18 GHz, compared with that at 2 GHz.

1. Introduction

It is anticipated that to provide realistic coverage at frequencies above 6 GHz, increased obstruction loss with respect to that at 2 GHz will have to be avoided by using beam steering at user locations to take advantage of lower-loss radio paths around obstructions via "reflectors of opportunity." Simultaneously, the extra transmission loss at higher frequencies that results from the smaller effective areas of higher-frequency antennas can be mitigated using the greater antenna gains that are concomitant with antennas that have steerable narrow beams.

The experiments reported herein were conducted to first determine if, in fact, beam steering could reduce excess losses at the higher frequencies in cluttered environments to values near those that one would expect in free space. This was found to be true, with excess losses reduced to less than 6 dB with respect to free space loss at 18 GHz. Measured results were also used to model transmission loss between unity gain antennas, L_{UGA}, and shadow loss. Simulations were then conducted based on these models, to determine 4x4 multi-user D-MIMO capacities that would be available in the same room, at 2 GHz, 18 GHz and 28 GHz, given a location-averaged SNR of 10 dB in each frequency band.

2. Measurements

The measurements were conducted using an Anritsu Model 37397C VNA, sweeping a bandwidth of 500 MHz, in 2 MHz steps. The power at the Tx port output was – 7 dBm, and this port was connected to the Tx antenna using 5 m of UFB142A-0 low loss transmission line. The receive antenna was connected to the receive port of the VNA using 3 m of EZFlex transmission line, which similarly has very low loss. For scenario #1, (Sc1), at 2 GHz the Tx antenna was an AINFO 2-18 GHz dual-polarised horn, with an H plane beamwidth of 27 deg and an E plane beamwidth of 35 deg. For this scenario, a 2-18 GHz omni directional biconical antenna at desk-height was used at the receiver, emulating a typical 2 GHz UE antenna. For Sc2, at 18 GHz and Sc3, at 28 GHz, the Tx antenna was an AINFO dual-polarised 18-40 GHz horn antenna. This antenna had an H-plane beamwidth of 44 deg. and an E-plane beamwidth of 51 deg. at 18 GHz and H and E plane beamwidths of 31 and 35 deg., respectively, at 28 GHz. The Tx horns were mounted at the end of the room, at the middle of the end wall, and at a height of 4 m above floor level, with a downtilt of 62.5 deg. to emulate a sector coverage antenna. Even with the different beamwidths at different frequencies, the Tx horns illuminated the total floor area of the study room within their 3 dB beamwidths in all 3 frequency bands. These horns were connected via their vertical polarisation feed. The 2-18 GHz horn was used as the receive antenna at 18 GHz, and a standard gain horn was used for receiving at 28 GHz. Both the latter horn antennas had beamwidths of approximately 10 deg. in both planes. A preamplifier that had gains of 0 dB at 2 GHz, 21.5 dB at 18 GHz, and 27 dB at 28 GHz was inserted in the receive transmission line as close to the receive antenna as possible. The Rx horn antennas were mounted on a remotely controllable pan/tilt platform and were scanned in 10 deg steps in azimuth from -180 to +170 deg with respect to the perpendicular direction towards the end wall where the Tx antenna was installed, and in elevation from -50 deg to +60 deg with respect to horizontal.

The room in which the measurements were conducted had dimensions of 5 m long × 3.6 m wide × 4 m high, with a concrete floor, a concrete ceiling at the 4-m height, and walls made of plasterboard mounted on galvanised steel studs separated from each other by 48.26 cm. The room also had a suspended ceiling at a height of 2.74 m, comprised of soft tiles hung within a metal grid, which also supported air conditioning vents and lighting fixtures.

3. Data analysis and results

For the analysis of transmission loss, insertion loss measurements from the calibrated VNA system and Tx lines were adjusted for antenna gains, and analysed as L_{UGA}, values, so they could later be used with any antenna gains of interest in systems calculations. Antenna gains, and pointing angles were all considered in these calculations. At each measurement location, and at 18 and 28 GHz, for each Rx antenna pointing direction, values of L_{UGA} were calculated as averages across the 500 MHz bandwidth swept by the VNA for the mitigation of received power variations caused by multipath propagation. As a system calibration check and verification of methodology, measurements that were made along the centreline of the room when it was empty were compared with results from ray tracing assuming single-interactions and horizontal propagation. These showed excellent agreement with the frequency-averaged measurement results, and were within fractions of a dB from results obtained using Frii's equation.

For each of the measurement scenarios, frequency-averaged values of L_{UGA} were plotted as a function of the logarithm of the direct-path Tx-Rx antenna separations, and fit to a linear model using standard LMS regression analyses. Fig. 1 shows the results for Sc2 at 18 GHz with the Rx antenna pointing in the direction of maximum received power, along with results from Frii's equation.

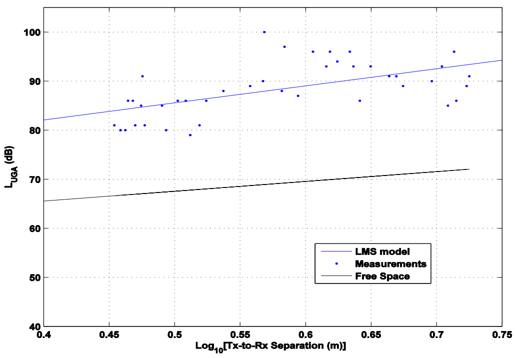

Fig. 1 Transmission loss at 18 GHz vs Tx/Rx antenna separation.

The slope of the model in Fig. 1 is 35 and its reference loss value is 84 dB at a range of 2.8 m. The sample CDF for shadow loss variations with respect to this model is shown in Fig. 2, along with a Gaussian (log normal when the random variable has values in decibels) model, having zero mean and a standard deviation of 4.3 dB. This model was verified to be a good fit to the sample CDF using the One-sample Kolmogorov-Smirnov test. Corresponding equations for these 18 GHz models can be written as:

$$L_{UGA_{18GHz}} = 84 + 35log_{10}(\frac{d}{2.8}) \tag{1a}$$

and

$$L_{SH_{18GHz}} = N(0,4.3\ dB). \tag{1b}$$

A similarly-derived model for the 2 GHz scenario can be written as

$$L_{UGA_{2GHz}} = 56 + 43log_{10}(\frac{d}{2.8}), \tag{2a}$$

and

$$L_{SH_{2GHz}} = N(0,5\ dB). \tag{2b}$$

The 28 GHz model values are not available at the time of writing, as the required measurements had not yet been completed. They will be included in the symposium presentation.

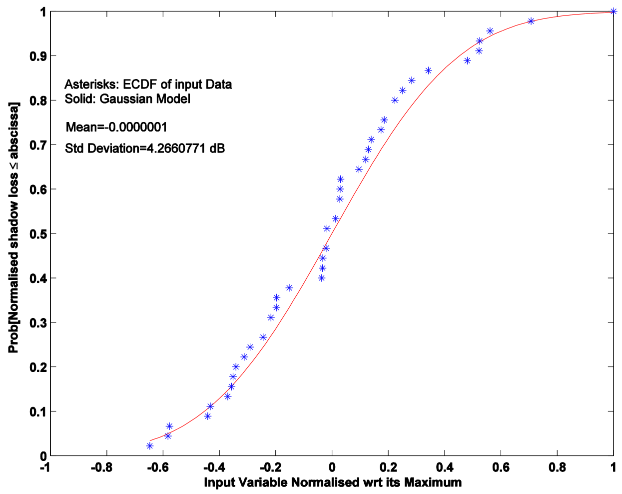

Fig. 2 Sample CDF for shadow loss variations wrt the average transmission loss model at 18 GHz, with a Gaussian model selected using the method of moments.

4. D-MIMO capacity calculations

4x4 multi-user D-MIMO capacities were calculated from simulations conducted assuming 4 remote radio heads (RRHs) at a 4-m height in the centre of each wall of a room the same size as the room where the measurements were made, and 4 users with quarter-wavelength monopole antennas at 2 GHz, and steerable narrow beam antennas having the same 10 deg. beamwidths as the measurement antennas at 18 GHz and 28 GHz. Further, it was assumed that the steerable antennas are capable of steering 4 beams, to receive the maximum power available at any particular Rx location, from each of the RRHs.

For the capacity calculations, MIMO matrices were constructed that had entries with uniformly random phases on [0, 2π], and magnitudes given by

$$|H_{ij}| = \sqrt{L_{UGA}(d_{ij}) + \Delta L_{SH} + \Delta L_{FF}}, \qquad (3)$$

where, the L_{UGA} values were determined from equations 1a 2a, and the equivalent for 28 GHz, with d_{ij} determined from the x and y coordinates of UEs, generated as uniform random variables over intervals corresponding to the dimensions of the room. The values of ΔL_{SH} were generated as decibel values from a Gaussian distribution, having means of zero and standard deviations as per equations 1b, 2b, and the equivalent for 28 GHz, and the values for $\Delta_{L_{FF}}$ were generated as the square of Rayleigh-distributed random variables. One thousand realisations were used. Fig. 3 shows capacity CDF results for a mean SNR of 10 dB, for scenario Sc1 at 2.4 GHz.

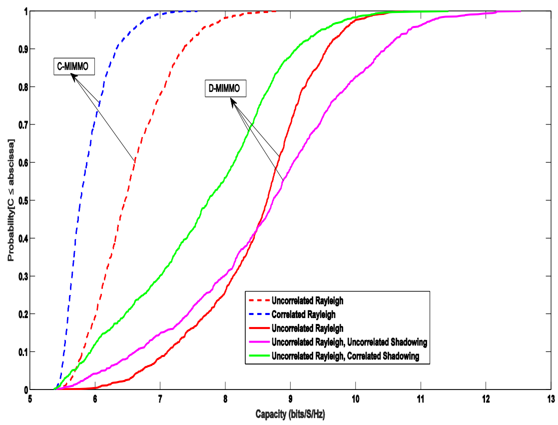

Fig. 3 Capacity CDFs generated from simulations based on propagation models derived from the 2.4 GHz measurements.

The curves labeled C-MIMO in Fig. 3 are equivalent results for conventional single-user MIMO, generated from the D-MIMO simulations by positioning the single user in the centre of the room for all 1000 realisations. As per the legend in the figure, there is a CDF for the D-MIMO case when there are only uncorrelated "fast fading" variations, one for when there uncorrelated fast fading variations and uncorrelated shadowing variations, and one for the case when there are uncorrelated fast fading variations and correlated shadowing variations. The shadowing correlation coefficient was set equal to a high value of 0.9 so the effect of shadowing correlations would be clearly visible. It can be seen that the D-MIMO results are as would be expected, with the shadowing variations "stretching" the capacity range represented by the CDF, and the shadowing correlations having the effect of decreasing capacity values.

Fig. 4 shows capacity results for Sc2, at 18 GHz.

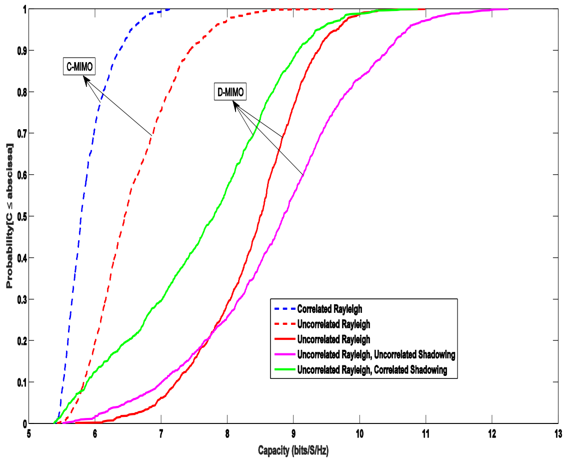

Fig. 4 Capacity CDFs generated from simulations based on propagation models derived from the 18 GHz measurements.

A comparison of the capacity CDFs in Figs. 3 and 4 shows considerable similarity, even though there was beam steering at the UE locations at 18 GHz, whereas the UE antennas were omnidirectional at 2.4 GHz. If the link budgets were arranged to give average SNRs of 10 dB in both frequency bands, under the condition of uncorrelated Rayleigh fast fading and uncorrelated shadowing, the median and maximum capacities would be equal. This indicates that the variations among the MIMO channel matrix elements for this case are dominated by the differences in the direct Tx/Rx path lengths, which were calculated from the x and y coordinates for UEs that were generated before the capacity calculations and recalled, so as to be the same for all realisations, for both frequency bands. Since results from the experiments at 18 GHz show that nearly equal received powers can be received from multiple directions, it is considered probable that beams could be steered to eliminate shadowing correlations at 18 GHz, whereas this would not be possible with omni directional antennas at the UEs at 2.4 GHz. Under such conditions, it would be appropriate to compare the capacity CDF for correlated shadowing at 2 GHz, with that for uncorrelated shadowing at 18 GHz, a comparison that shows a median capacity of 7.7 bits/S/Hz at 2 GHz under heavily correlated shadowing and, a median of 8.8 bits/S/Hz at 18 GHz under uncorrelated shadowing, given equal SNRs of 10 dB averaged over the coverage area. The propagation measurement results show that, in order to achieve equal average SNRs for the cited scenarios at 2 GHz and 18 GHz, an additional gain of about 25 dB is needed in the link budget for 18 GHz. This is only about 6 dB more than the ratio that would be required in free space, and demonstrates that excess obstruction loss in the higher frequency bands can be significantly reduced through the use of beam steering.

5. Acknowledgements

The authors would like to express their gratitude to NSERC Canada, Ericsson Canada, and Mitacs Canada for their financial and in-kind support of research upon which the results in this paper are based.